Title: Characterization of Stainless Steel Surfaces - Modified in air at 350°C

Authors: Mari Honkanen, Minnamari Vippola and Toivo Lepistö

Postal address for all authors: Department of Materials Science, Tampere University of Technology, P.O.B. 589, FIN-33101 Tampere, Finland

Authors' E-mails: Mari Honkanen: mari.honkanen@tut.fi

Minnamari Vippola: minnamari.vippola@tut.fi

Toivo Lepistö:toivo.lepisto@tut.fi

Corresponding author: Mari Honkanen (tel: +358408490133, fax: +358331152330)

ABSTRACT

This work aimed to modify stainless steel surface by oxidation for metal-plastic hybrid applications. Oxidation behaviour of the stainless steels AISI 304 and 316L was studied by TEM and AFM. Air exposures for steels were carried out in air at 350 °C for 5-300 minutes. The oxide layer structures were characterised by planar and cross-sectional TEM samples. Behaviour of the both steels was very similar. Oxidation started already during first 5 minutes and a protective oxide layer formed fast and further oxidation was slower. Oxide structures were mainly of the type M_2O_3. Surface topography of the oxide layer was studied by AFM. At first, single oxide islands formed on the base oxide layer. After 100 and 300 minutes exposures, the islands have combined to the thin, uniform, and dense oxide layer. Due to this, an optimal stainless steel insert surface for metal-plastic hybrid parts would be after those treatments.

KEYWORDS

Stainless steel; Oxidation; Metal-plastic hybrid; Transmission electron microscopy; Atomic force microscopy

1. INTRODUCTION

Austenitic stainless steels are used in almost all types of industries. According to that, also the oxidation phenomenon of stainless steels is interesting subject even if they have very good corrosion resistance. Corrosion resistance of stainless steel is based on a thin chromium oxide film forming on the steel surface and protecting the under-laying material for further oxidation. The presence of oxygen is essential to the formation of the protective film. This passive film forms spontaneously and immediately in the presence of oxygen. Further oxidation depends on the transport of metal and oxygen atoms or ions through the oxide layer. For example, the increase of temperature or a chemically aggressive environment increases atom and ion diffusivity through the oxide layer and due to that, the thickness of the oxide layer start to grow. At room temperature, the native oxide layer on stainless steel is typically 1–3 nm thick. This is due to the fact that the mobility of the atoms and ions is insignificant and thus the oxide film growth stops. The thin passive layer grows within seconds, while the long range ordering of the layer is a slower process lasting typically several hours. The formed oxide film is self-repairing in oxygen containing environments. Under certain circumstances the passive layer, however, destroys permanently and catastrophical corrosion may occur. The best corrosion resistance will be gained when the steel is boldly exposed and the surface is free of deposits. [1-5]

Several studies indicate that the oxide layer on stainless steel has a complex and multi-layer structure. [5-12] The oxide film consists theoretically of the wide array of the oxides e.g. Fe_2O_3, Cr_2O_3, $FeCr_2O_4$, Fe_3O_4, and FeO. The most common oxides are Fe_2O_3 and

Cr_2O_3. The microstructure and the growth of the oxide scales depend on many factors, like: oxidation time, temperature, environment, and alloying elements. The oxide layer just above the steel-oxide interface is usually Cr-rich and the layer above that, riches in Fe. There are also low-oxygen layers between the oxygen-rich ones formed due to internal oxidation of the steel. The passive film consists mainly of chromium oxide (Cr_2O_3). [5,6,13]

N. Karimi et al. [12] studied oxides on AISI 304 formed in air at 1000 °C. They noticed that during first 10 hours, an oxide layer grows outwards and consists of $Mn_{1.5}Cr_{1.5}O_4$ and Cr_2O_3. Between 10 and 12 hours, iron diffuses through the oxide scale and Cr_2O_3 transforms to $FeCr_2O_4$. In addition, Fe_2O_3 forms at the air/oxide –interface. [12] Those iron containing oxides are not considered as protective as chromia oxides. [14] H. Buscail et al. [14] compared oxidation behaviour of AISI 304 and AISI 316L in same conditions than N. Karimi et al. [12], in air at 1000 °C. They noticed that the oxidation behaviour of AISI 316L was better than that of AISI 304 considering kinetics and structural characteristics. They assumed that molybdenum in AISI 316L is a protective component and it prevents the diffusion of the iron atoms to the air/oxide –interface in which case, the oxide layer is mainly the type of the protective Cr_2O_3, not non-protective iron containing oxides. [14,12]

The aim of this work was to modify stainless steel surfaces by oxidation for metal-plastic hybrid applications. Good properties of totally different materials can be combined in metal-plastic hybrid parts. Manufacturing of the hybrid parts is not, however, easy because of metals and plastics have very different physical and chemical

characters. This usually causes poor adhesion between metal and plastic, shrinkage of plastic, residual stresses, and therefore, bending of the hybrid parts. [15-17] Adhesion between two or more distinct constituents, such as metal and plastic, can be improved by using coupling agents. Silicon based chemicals silanes are the most commonly used coupling agents to bond organic materials to metals or metal oxides. [18] Modification of the metal surface can influence the adhesion of silane onto the metal surface. This has been noted especially in the case of aluminium. Susac et al. [19] have studied the adhesion of organosilane on 2024-T3 aluminum alloy. Mechanically polished fresh and air exposed (20 hours) samples were used in the silane treatment. They noticed that the adhesion of silane onto the fresh polished sample was poor while, the adhesion of the silane onto the air exposed sample was good. [19] In addition, Kim et al. [20] have studied the adhesion of two organosilanes onto the different microstructural regions of 7075-T6 aluminum alloy as well as the effect of the heating pre-treatment on silane adhesion. Samples were air-exposed or heat-treated in air at 200 °C. In the case of the air exposed samples, surface microstructure (second-phase particles and matrix) influenced adhesion. During heat treatment at 200 °C, oxides grew on the second-phase particles and matrix. After this heat treatment silane formed a uniform layer onto the oxide layer of the aluminum. [20] This means that formation of a uniform and smooth oxide layer on the metal surface is likely essential to quarantee a good adhesion between metal and plastic. In addition of aluminum, stainless steel is an interesting material choice for metal-plastic hybrid applications because stainless steel is widely used in several applications. Therefore, in this work, oxidation phenomenon of the stainless steels AISI 304 and AISI 316L was studied to achieve the most optimal oxidized surface for silane adhesion to stainless steel surface. Air exposures were carried out in air at 350 °C for 5-

300 minutes. The oxide layer structures were characterised by transmission electron microscope (TEM) with planar and cross-sectional samples and surface topography of the oxide layers was studied by atomic force microscope (AFM).

2. MATERIALS AND EXPERIMENTAL

Two commercial stainless steel grades (Outokumpu) were characterised. The steel grades were AISI 304 and AISI 316L which is an acid-proof steel and contains also molybdenum. The chemical compositions and designations of these steels are presented in Tab. 1. [2] In this article, ASTM steel names are used. The steels were received in a plate shape with an average grain size about 15 μm.

The oxidation treatments were carried out in air in a ceramic tube furnace at 350 °C. The oxide layers formed on the stainless steels were studied from two directions by TEM (Jeol, JEM 2010): from above (planar samples) and from cross-section. Exposure times for the planar TEM samples were 5, 25 and 100 minutes and for the cross-sectional TEM samples 100 and 300 minutes. Also the fresh sample was studied.

The planar TEM samples for the oxidation treatments were prepared with twin jet electrolytical polisher (Struers, Tenu-Pol-5) using a solution of nitric acid in methanol (1:2) at -50 °C. Pre-thinning before electropolishing was made mechanically to 0.1 mm thickness and then 3 mm diameter discs were cut with the punch (South Bay Technology Inc., Model 310) from the pre-thinned samples for final thinning and

polishing. The just polished fresh and air-exposed planar samples were studied with TEM. The same area of the sample was located and the same beam direction **B**=[1,1,2] was used after each oxidation treatments (5, 25 and 100 minutes). Thus, the same area of the sample was always searched in TEM after each oxidation treatments and it was always tilted to the same direction. The same area was found with very careful mapping of the sample.

Samples for the cross-sectional TEM studies of oxide layers were prepared by using method described in Ref. 21. The small pieces were cut from recrystallised plates with a diamond saw (Technoorg – Linda, Microsaw^{TM}). The specimens were ground mechanically to size ~1.7 mm x ~1 mm x ~0.4 mm. The ground specimens were air-exposed in a furnace at 350°C for 100 and 300 minutes. Two exposed pieces were embedded into a titanium grid so that the exposed surfaces were face-to-face. The samples were attached into the grid by carbon-araldite glue. The glued grid was pre-thinned by hand to thickness of ~100 μm and then with dimple grinder (Gatan Inc., Model 656) to the thickness of ~20 μm. The final thinning was made with precision ion polishing system (PIPS, Gatan Inc., PIPS Model 691).

AFM samples were cut off from the electrolytically polished (JaloteräsStudio, West Lapland Vocational) AISI 304 plate for dimensions of about 10 mm x 10 mm. The fresh and 5, 25, 100 and 300 minutes air exposed samples were studied by AFM (Veeco, Dimension 3100 AFM, Nanoscope IVa) in the tapping mode with a scan rate 0.5 Hz and scan area 2 μm x 2 μm.

3. RESULTS AND DISCUSSION

3.1. TEM results

The oxide structures of stainless steels were characterised by planar and cross-sectional TEM samples. Thus, the oxide layers were studied from two directions: from above (planar samples) and from cross-section.

3.1.1. Planar TEM samples

Oxidation treatments were carried out in air at 350 °C for 5, 25 and 100 minutes. The same area of the sample was always studied in TEM after each oxidation treatment and it was always tilted to the same direction. TEM images and selected area electron diffraction (SAED) patterns of the AISI 304 and AISI 316L before and after each oxidation treatment are presented in Figs. 1 (a) - (d) and Figs. 2 (a) - (d), respectively. Based on SAED patterns, oxidation started already during the first 5 minutes and the patterns indicated the nanocrystalline structure of oxide. The enlargement SAED-patterns of the AISI 304 and AISI 316L after 100 minutes exposure in air at 350 °C are presented in Fig. 3. The lattice plane spacing values of e.g. Cr_2O_3, Fe_2O_3, FeO, and NiO are very close to each other and therefore, identification of the oxide structures with the ring pattern was not possible. Multi-layer structure and the thinness of the oxide layers complicated further the structure determination. The d-values of the rings and the possible oxide structures with these d-values are marked in Fig. 3. Those ED-patterns

indicate that the oxide structures were mainly of the type M_2O_3. This agrees well with the findings in literature. [5,6,13] Behaviour of the both steels AISI 304 and AISI 316L was very similar in these testing conditions.

3.1.2. Cross-sectional TEM samples

The cross-sectional TEM samples from air exposed pieces were prepared to get more information about the thickness and structures of the oxide layers. Based on the oxidised planar samples, the oxide layers were very thin even after 100 minutes exposure, therefore the cross-sectional samples were exposed for 100 and 300 minutes. The cross-sectional sample preparation was very challenging with earlier described method. The steel oxidised and reacted with the glue during ion polishing process. Due to that, a crystalline layer formed on the sample.

Cross-sectional TEM images after oxidation treatment in air at 350 °C are presented in Figs. 4 (a) AISI 316L for 100 min and (b) AISI 304 for 300 min. The oxide layers were very dense and adhesion onto base metal was good. After 100 minutes oxidation, thickness of the oxide layer was about 15 nm and after 300 minutes oxidation it was about 18 nm. Based on the planar and cross-sectional TEM studies, at first, oxidation occurred very fast and after 100 minutes the growing of the oxide layer was slower, thus a protective oxide layer formed fast onto studied stainless steels in the tested conditions.

According to SAED patterns and cross-sectional TEM images, the oxide structures and oxidation kinetics of both steels were very similar. Differences in oxide structures were not observed such as N. Karimi et al. [12] and H. Buscail et al. [14] noted in their studies that were carried out in air at 1000 °C. According to our and their studies, differences in oxidation behaviours between AISI 304 and AISI 316L can be detected at very high temperatures with long exposure times where in AISI 316L has more protective oxide layers but in low temperatures, both stainless steels have similar oxidation behaviour.

3.2. AFM results of AISI 304

Topography of the electrolytically polished fresh and oxidised AISI 304 was studied by AFM. The samples were exposed in air at 350 °C for 5, 25, 100 and 300 minutes. AFM images of the fresh and oxidised samples are presented in Figs. 5 (a) - (e). Stainless steels form a thin passive layer fast and spontaneously in the presence of oxygen [7,10] so the fresh sample has a very thin base oxide film. AFM image of the fresh sample (Fig. 5 (a)) indicated also some oxide islands on this base oxide film. During 5 and 25 min exposures, number of these oxide islands increased (Figs. 5 (b) and (c)). After 100 and 300 min. exposures, the islands have combined to the uniform oxide layer.

Surface topographies of the 5, 25, 100 and 300 min exposed samples are presented in Figs. 6 (a) - (d). Based on topographies of the 5 and 25 min exposed samples, single about 18 nm height and 200 nm width islands formed on the base oxide layer. After 100 min exposure, the flat islands covered the surface and they formed a uniform layer.

Topography of the oxide layer changed between 100 and 300 min. exposure, resulting the pointed shape of the islands after 300 min. exposure.

4. CONCLUSIONS

The aim of this work was to modify stainless steel surfaces by oxidation for metal-plastic hybrid applications. Oxide layer structures and topography of oxide layers on the AISI 304 and AISI 316L were studied by TEM and AFM. Air exposures were carried out at 350 °C for different times between 5 and 300 minutes. Planar and cross-sectional samples were prepared for TEM studies. Behaviour of the both steels AISI 304 and AISI 316L was very similar in testing conditions. Based on the planar TEM sample studies, nanocrystalline oxide layer growth started already during the first 5 minutes. Definite determination of the oxide structures was not possible but the ED-patterns indicated that the oxide structures were mainly of the type M_2O_3. More surface effective methods, such as X-ray photoelectron spectroscopy (XPS), would be needed to the exact identification of the oxide structures formed at low temperatures. Cross-sectional TEM samples were prepared from 100 and 300 min exposed samples. The oxide layers were very dense. Thickness of the oxide layers after 100 min exposure was about 15 nm and after 300 min about 18 nm. Based on these TEM studies, a protective oxide layer formed fast and further oxidation was slower. Topography of the polished fresh and exposed AISI 304 samples was studied by AFM. After 5 and 25 min exposures, single oxide islands formed on the base oxide layer and after 100 and 300 min exposures, the

islands have combined to the uniform oxide layer. Shape of the oxide islands changed according to exposure times.

After oxidation treatment in air at 350 °C for 100 or 300 minutes, the oxide layer was dense and uniform. According to this, an optimal stainless steel insert surface for metal-plastic hybrid parts would be after those treatments. Our further studies of the hybrid parts will establish how surface topography of the oxide layer improves metal-coupling agent adhesion and thus metal-plastic adhesion.

ACKNOWLEDGEMENTS

The authors gratefully thank The National Technology Agency of Finland (TEKES) and The Graduate School of the Processing of Polymers and Polymer-based Multimaterials (POPROK) for financial support.

References:

[1] B. Leffler: ‘Stainless - stainless steels and their properties’, www.outokumpu.com/files/Group/HR/Documents/STAINLESS20.pdf.

[2] www.outokumpu.com.

[3] R. Davison, T. DeBold and M. Johnson: in ‘Metals Handbook’, (ed. L. Korb *et al.*), vol. 13, 549-550; 1987, Ohio, Metals Park.

[4] C. Olsson and D. Landolt: *Electrochimica Acta*, 2003, **48**, 1093-1104.

[5] J. Tang, M. Halvarsson, H. Asteman and J.-E. Svensson: *Micron*, 2001, **32**, 799-805.

[6] W. Zielinski and K. Kurzydlowski: *Scripta Materialia*, 2000, **43**, 33-37.

[7] A. Vesel, M. Mozetic and A. Zalar: *Applied Surface Science*, 2002, **200**, 94-103.

[8] A. Johnson, D. Parsons, J. Manzerova, D. Perry, D. Koury, B. Hosterman and J. Farley: *Journal of Nuclear Materials*, 2004, **328**, 88-96.

[9] F. Shieu, M. Deng and S Lin: *Corrosion Science*, 1998, **40**, 1267-1279.

[10] M. Halvarsson, J. Tang, H. Asteman, J.-E. Svensson and L.-G. Johansson: *Corrosion Science*, 2006, **48**, 2014-2035.

[11] K. Nomura and Y. Ujihira: *Journal of Materials Science*, 1990, **25**, 1745-1750.

[12] N. Karimi, F. Riffard, F. Rabaste, S. Perrier, R. Cueff, C. Issartel and H. Buscail: Applied Surface Science, 2008, **254**, 2292-2299.

[13] S. Birosca and R. L. Higginson: *Materials at High Temperatures*, 2005, **22**, 179-184.

[14] H. Buscail, S. El Messki, F. Riffard, S. Perrier, R. Cueff, E. Caudron, C. Issartel: Materials Chemistry and Physics, 2008, **111**, 491-496.

[15] P. Fabrin and M. Hoikkanen, In: 'Proceedings of SPE Annual Technical Conference (ANTEC 2007)', 2528-2532, 2007, Cincinnati, USA.

[16] G. Zhao and G. Ehrenstein, In: 'Proceedings of SPE Annual Technical Conference (ANTEC 1999)', 1332-1336, 1999, New York, USA.

[17] O. Zoellner and J. Evans, In: 'Proceedings of SPE Annual Technical Conference (ANTEC 2002)', 1-4, 2002, San Fransisco, USA.

[18] E. Plueddemanm: ‘Silane coupling agents’, 235; 1982, New York, Plenum Press.

[19] D. Susac, X. Sun and K. Mitchell: *Applied Surface Science*, 2003, **207**, 40-50.

[20] J. Kim, P. Wong, K. Wong, R. Sodhi and K. Mitchell: *Applied Surface Science*, 2007, **253**, 3133-3143.

[21] M. Honkanen, M. Vippola and T. Lepistö: *Journal of Materials Research*, 2008, **23**, 1350-1357.

Table:

Table 1. Chemical compositions and designations of studied steels. [2]

Steel designations			Typical chemical composition [%]			
Outokumpu steel name	EN	ASTM	C (max)	Cr	Ni	Mo
4301	1.4301	AISI 304	0.07	17.5	8	-
4404	1.4404	AISI 316L	0.03	16.5	10	2

Figure captions:

Figure 1. TEM images and SAED patterns of AISI 304 (a) before oxidation treatments, (b) after 5 min, (c) after 25 min, and (d) after 100 min oxidation in air at 350 °C.

Figure 2. TEM images and SAED patterns of AISI 316L (a) before oxidation treatments, (b) after 5 min, (c) after 25 min, and (d) after 100 min oxidation in air at 350 °C.

Figure 3. SAED patterns of AISI 304 and AISI 316L after oxidation in air at 350 °C for 100 minutes. D-values of some rings are marked and also possible oxide structures with these d-values.

Figure 4. Cross-sectional TEM images after oxidation treatment in air at 350 °C (a) AISI 316L for 100 min and (b) AISI 304 for 300 min.

Figure 5. AFM images of (a) fresh, industrially polished AISI 304, (b) 5 min oxidised at 350 °C, (c) 25 min oxidised at 350 °C, (d) 100 min oxidised at 350 °C, and (e) 300 min oxidised at 350 °C.

Figure 6. Surface topographies of AISI 304 (a) 5 min oxidised, (b) 25 min oxidised, (c) 100 min oxidised, and (d) 300 min oxidised in air at 350 °C.

Figure 1:

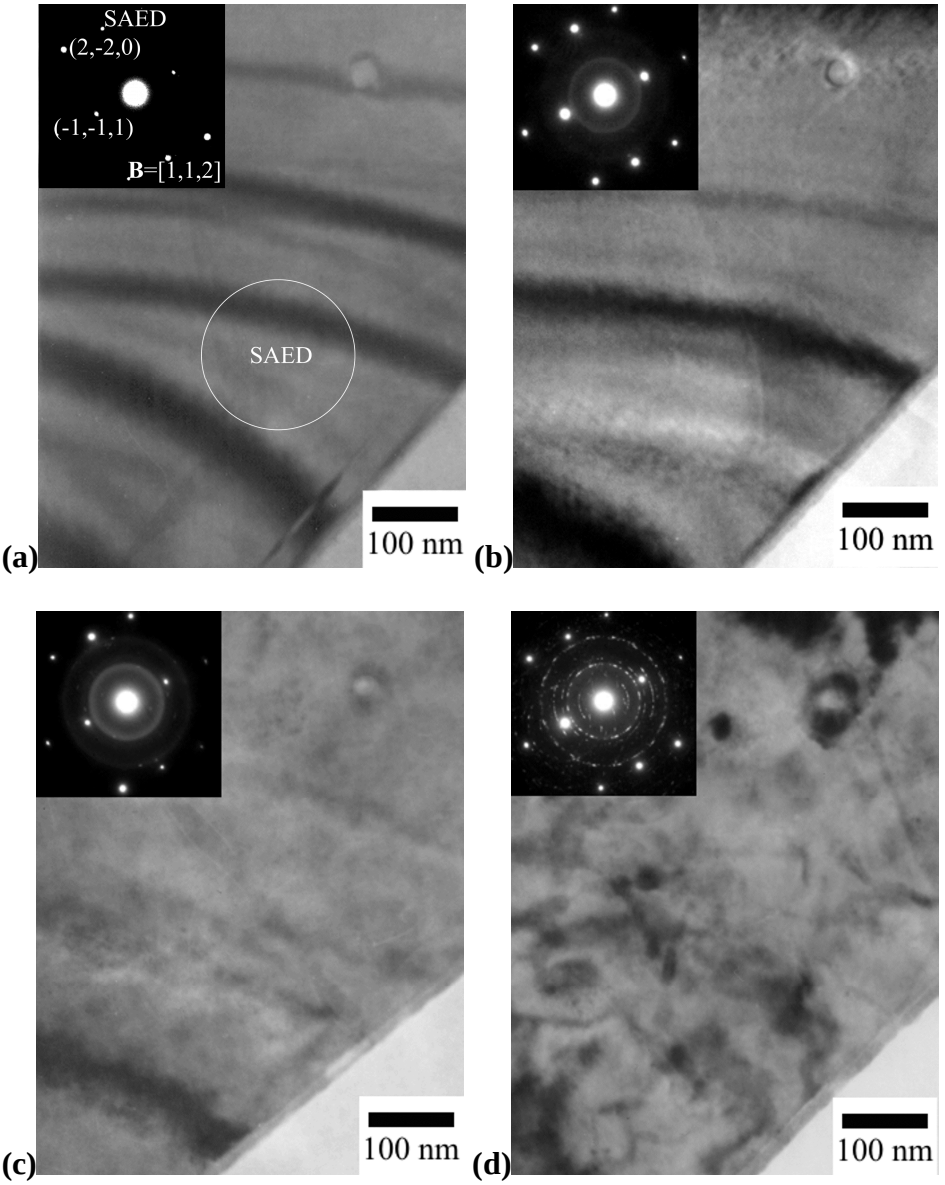

Figure 2:

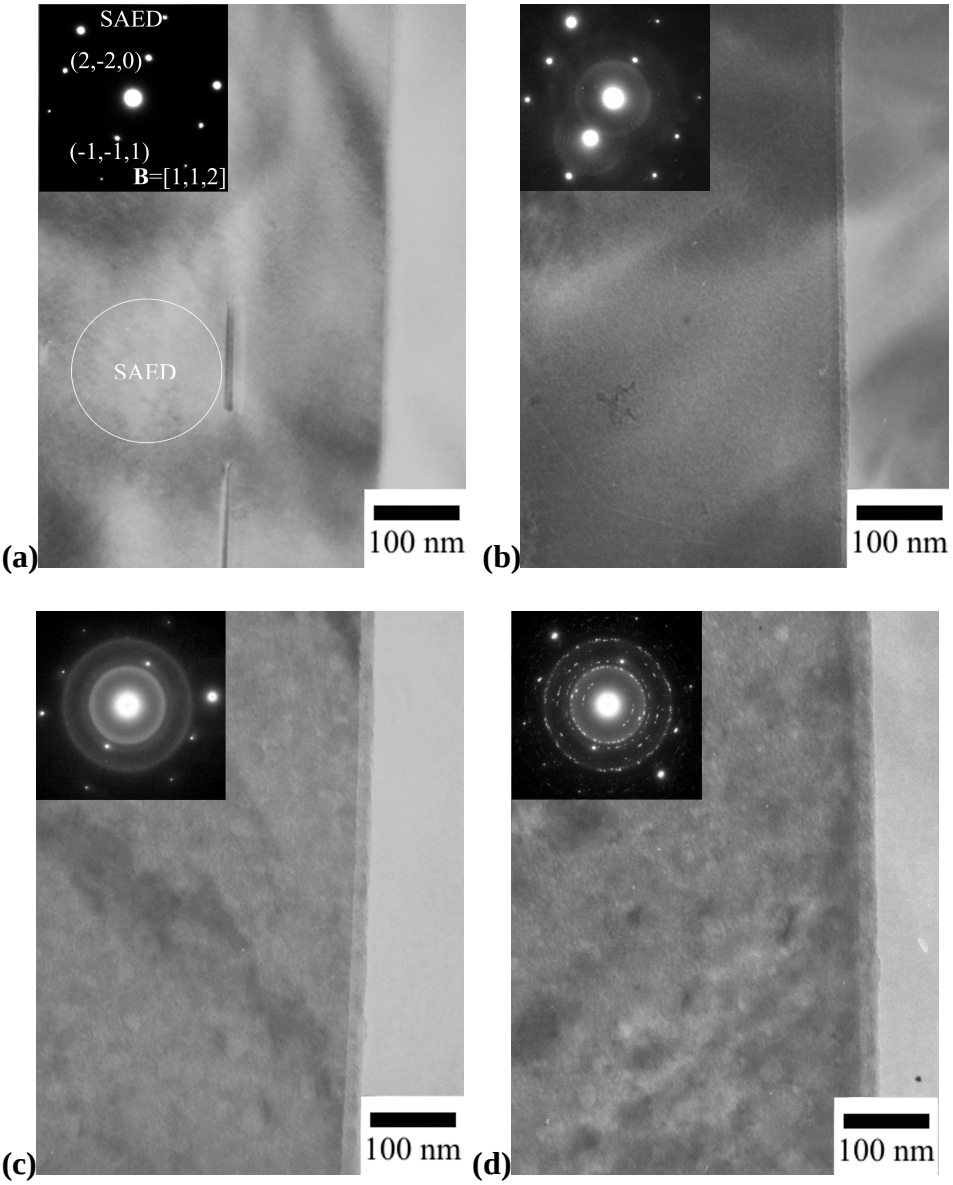

(a) **(b)** **(c)** **(d)**

Figure 3:

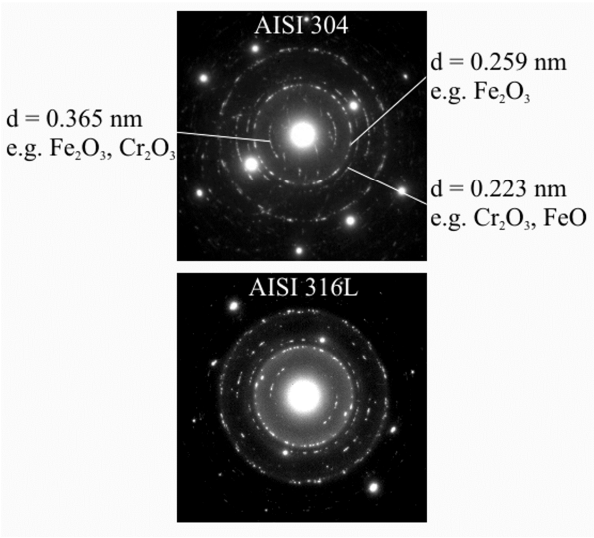
AISI 304
d = 0.259 nm
e.g. Fe_2O_3
d = 0.365 nm
e.g. Fe_2O_3, Cr_2O_3
d = 0.223 nm
e.g. Cr_2O_3, FeO
AISI 316L

Figure 4:

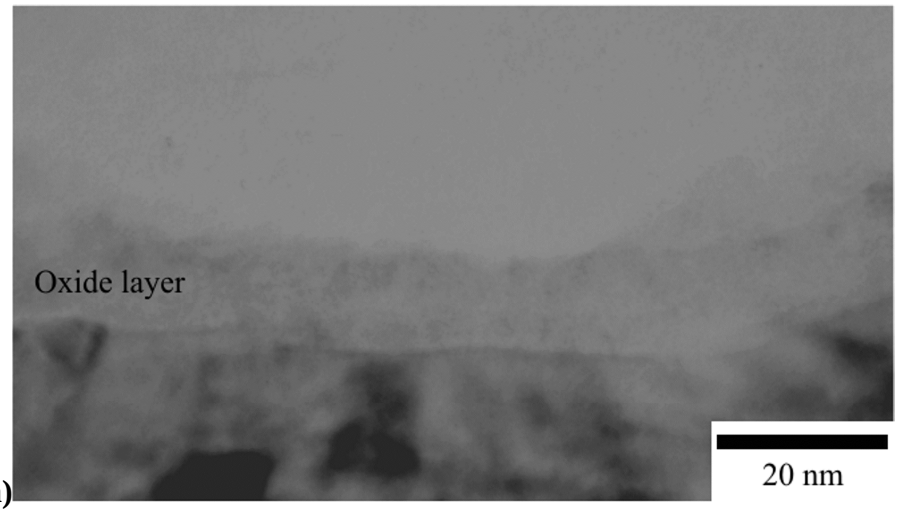

(a)

(b)

Figure 5:

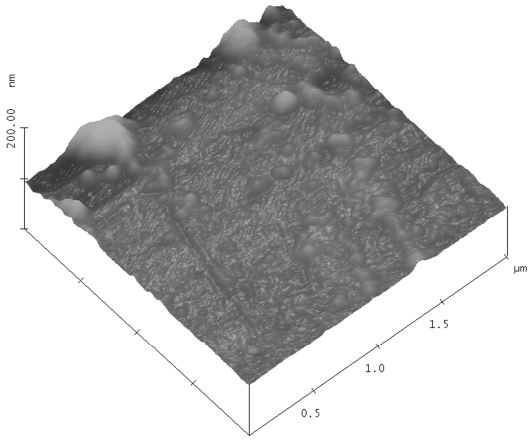

(a)

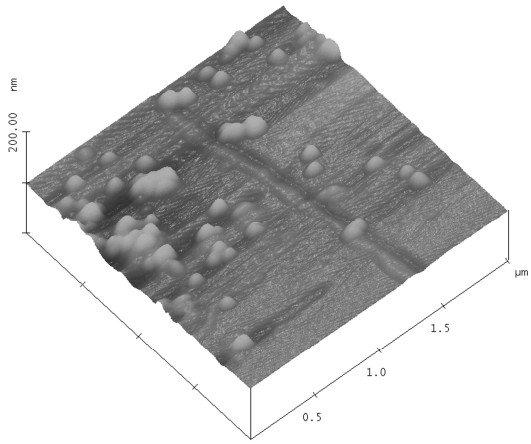

(b)

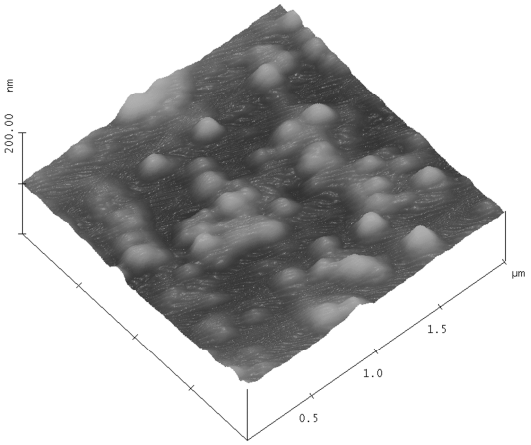

(c)

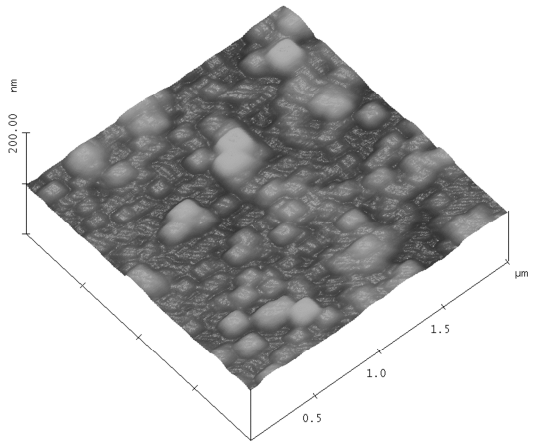

(d)

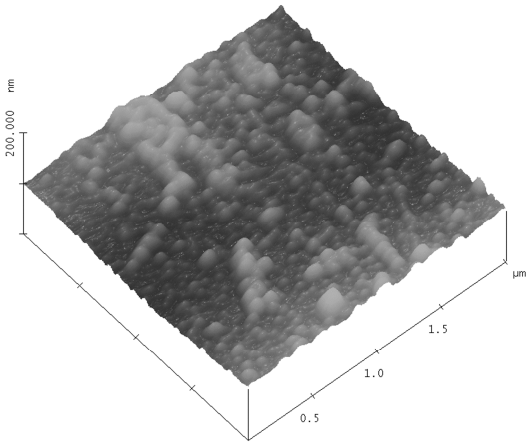

(e)

Figure 6:

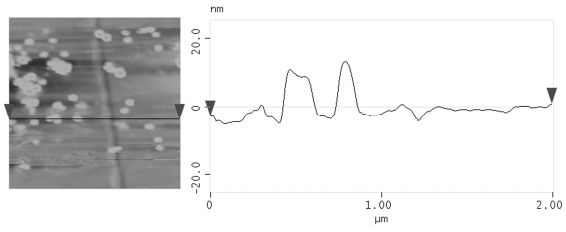

(a)

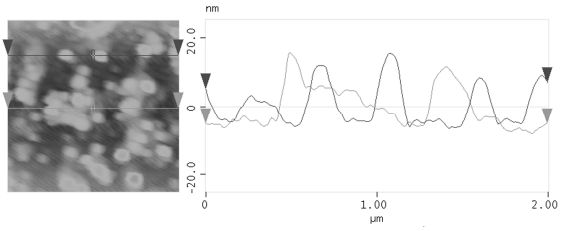

(b)

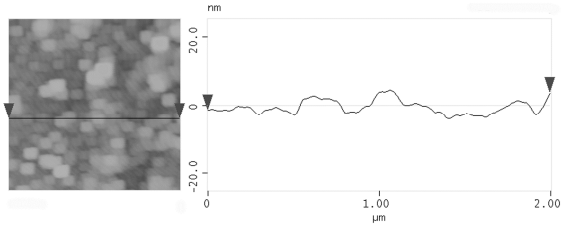

(c)

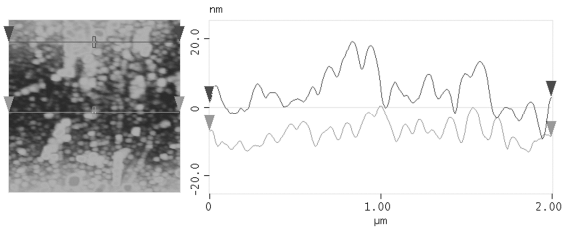

(d)